Downloaded from orbit.dtu.dk on: Mar 16, 2025

DTU Library

Clinical feasibility of a label-free SERS assay for therapeutic drug monitoring of methotrexate

Dumont, Elodie; Soufi, Gohar; Göksel, Yaman; Slipets, Roman; Raja, Raheel Altaf; Schmiegelow, Kjeld; Zor, Kinga; Boisen, Anja

Published in:
Sensing and Bio-Sensing Research

Link to article, DOI:
10.1016/j.sbsr.2024.100649

Publication date:
2024

Document Version
Publisher's PDF, also known as Version of record

Link back to DTU Orbit

Citation (APA):
Dumont, E., Soufi, G., Göksel, Y., Slipets, R., Raja, R. A., Schmiegelow, K., Zor, K., & Boisen, A. (2024). Clinical feasibility of a label-free SERS assay for therapeutic drug monitoring of methotrexate. *Sensing and Bio-Sensing Research*, *44*, Article 100649. https://doi.org/10.1016/j.sbsr.2024.100649

General rights
Copyright and moral rights for the publications made accessible in the public portal are retained by the authors and/or other copyright owners and it is a condition of accessing publications that users recognise and abide by the legal requirements associated with these rights.

- Users may download and print one copy of any publication from the public portal for the purpose of private study or research.
- You may not further distribute the material or use it for any profit-making activity or commercial gain
- You may freely distribute the URL identifying the publication in the public portal

If you believe that this document breaches copyright please contact us providing details, and we will remove access to the work immediately and investigate your claim.

Sensing and Bio-Sensing Research 44 (2024) 100649

Contents lists available at ScienceDirect

Sensing and Bio-Sensing Research

journal homepage: www.elsevier.com/locate/sbsr

Clinical feasibility of a label-free SERS assay for therapeutic drug monitoring of methotrexate

Elodie Dumont [a,b,*], Gohar Soufi [a,b,*], Yaman Göksel [a,b], Roman Slipets [a,b], Raheel Altaf Raja [c], Kjeld Schmiegelow [c], Kinga Zor [a,b], Anja Boisen [a,b]

[a] Center for Intelligent Drug Delivery and Sensing Using Microcontainers and Nanomechanics (IDUN), Department of Health Technology, Technical University of Denmark, Kgs. Lyngby 2800, Denmark
[b] BioInnovation Institute Foundation, Copenhagen N, 2200, Denmark
[c] Department of Paediatrics and Adolescent Medicine, Rigshospitalet University Hospital, Copenhagen 2100, Denmark

ARTICLE INFO

Keywords:
SERS
Methotrexate (MTX)
Silver nanopillars (AgNPs)
Method comparison
Chemometrics
Therapeutic drug monitoring (TDM)

ABSTRACT

We present a therapeutic drug monitoring (TDM) feasibility study using a label-free surface-enhanced Raman spectroscopy (SERS)-based assay for quantifying methotrexate (MTX) from samples collected from children with acute lymphoblastic leukemia undergoing high-dose MTX therapy. We show that, when combined with an appropriate sample preparation (solid phase extraction) and multivariate data analysis (partial least squares regression), the SERS assay demonstrated a good correlation with a reference chromatographic method ($r = 0.889$, $p < 0.005$). We also found that the SERS-based approach underestimated MTX concentration, with a 10% bias calculated, but both methods showed similar variability (RSD of 8.4% for HPLC and 11.6% for SERS). The presented results are strong evidence that SERS can be used for TDM of MTX, and this work brings us one step closer to implementing a SERS-based assay in clinics.

1. Introduction

Therapeutic drug monitoring (TDM) of methotrexate (MTX) during high-dose MTX (HD-MTX) therapy, a treatment frequently used in acute lymphoblastic leukemia, is of crucial importance to avoid fatal drug toxicities [1]. It is in particular critical to avoid toxicities related to high MTX blood levels [2] and to determine when to discontinue administrating MTX rescue drug [3]. Despite the need, TDM, even in this case, is carried out in centralized laboratories, which can delay action-taking due to logistical and analytical issues, such as shipping or analysis time. Regardless of its importance, TDM of MTX in some cases is not even accessible in some parts of the world, especially in low- and middle-income countries, which nonetheless encompass 80% of cancerous children globally [1]. Currently, MTX levels are monitored using immunoassays or chromatographic techniques, the latter being the gold standard [2,4]. Immunoassays in developed countries are usually conducted on large chemical analyzers [5,6], which enable a high level of automation; however, they have a substantial initial purchase cost, recurring kit purchasing costs, and the chemicals need refrigeration, which makes it rather complex and costly for certain parts of the globe. Besides, immunoassays are prone to possible interferences, such as metabolites [7,8].

On the other hand, chromatographic techniques require high initial financial investment and specifically trained personnel to operate the equipment, mainly during working hours. An additional burden linked to chromatography is the longer time-to-results [8,9].

This is why several initiatives exist to develop alternative approaches [7,10] to classical analytical methods and label-free analytical techniques, such as based on spectroscopic techniques for TDM. Surface-enhanced Raman spectroscopy (SERS) is one of those techniques that is gaining grounds for bioanalysis and is particularly well-suited for TDM purposes [11]. SERS is indeed label-free, has multiplexing abilities, and SERS assays have the potential to be miniaturized and automated [11,12]. However, despite those benefits, quantitative biomedical SERS assays are still not commercially available, and few SERS literature focuses on comparing SERS results with those obtained with reference methods [11,13]. Among various types of SERS substrates, nanopillar substrates have emerged as promising candidates due to their

* Corresponding authors: Center for Intelligent Drug Delivery and Sensing Using Microcontainers and Nanomechanics (IDUN), Department of Health Technology, Technical University of Denmark, Kgs. Lyngby 2800, Denmark.
E-mail address: gohsoo@dtu.dk (G. Soufi).

https://doi.org/10.1016/j.sbsr.2024.100649
Received 31 January 2024; Received in revised form 11 April 2024; Accepted 18 April 2024
Available online 19 April 2024
2214-1804/© 2024 The Authors. Published by Elsevier B.V. This is an open access article under the CC BY license (http://creativecommons.org/licenses/by/4.0/).

exceptional sensitivity and repeatability, as recently demonstrated by Feizpour et al. [14] Compared to colloidal silver or gold nanoparticles, nanopillar substrates exhibit significantly higher sensitivity and repeatability, attributed to the unique leaning effect and generation of strong hotspots. Some other works used other substrates, showing a higher quantification range than nanopillar substrates [12,15,16]. It's essential to consider the overall sensitivity and reproducibility offered by nanopillar substrates, which have been validated in various studies [14]. Additionally, while the fabrication of nanopillar substrates may require specific facilities like clean rooms, they offer the advantage of mass production (https://www.silmeco.com/) and reproducibility, making them available to all at an affordable price and therefore highly attractive for practical applications in SERS-based detection. On the other hand, nanoparticles are often produced in small batches and are prone to variations between laboratories [17]. In the context of TDM, the clinical validation of analytical methods is crucial to verify their accuracy, precision, reliability, and suitability for routine use [18–20], ensuring that the measured concentrations reflect the actual drug levels and are not affected by the presence of other endogenous substances or co-administered drugs [20]. Even though the number of studies involving clinical validation of discriminative diagnostic SERS assays is starting to increase [21–25], there is still a lack of clinical validation of quantitative ones, with, to the best of our knowledge, a single published research paper so far [13]. The limited availability of validation studies could be due to the combination of two factors: surface fouling and competition and reproducibility issues with the SERS substrate [26,27].

It is well known, especially regarding complex matrices, that SERS performances may be hindered by competition for the hot spots on the SERS substrate and surface fouling [28,29]. These issues are further multiplied in bioanalyses, where the typical biological variability of the samples, both in terms of intra- and inter-individual variability, is added on top of the previously cited challenges [26].

Herein, we report data from the quantification of MTX from samples collected from children with acute lymphoblastic leukemia undergoing HD- MTX therapy, comparing SERS-based quantification with a gold standard reverse-phase high-performance liquid chromatography (HPLC) method with a UV–visible detector.

A fast (10 min) sample clean-up step, a solid phase extraction (SPE) procedure miniaturized in a syringe filter [12], was introduced before SERS detection to circumvent surface fouling and competition. The SERS detection was conducted on silver nanopillar (AgNPs) substrates, according to the previously described nanopillar assisted separation (NPAS) process [30], which could additionally improve sample clean-up due to the structure of the AgNPs enabling sample migration and separation by capillary forces on the substrate [30].

Moreover, to account for possible spectral interferences originating from the high biological variability of the samples, spectral data were analyzed using multivariate data analysis, namely partial least squares regression (PLSR), to create quantitative models taking the whole spectrum into account. The detection (3 min) was conducted on a home-built portable Raman spectrometer, with the consideration and perspective to develop a SERS-based MTX assay that could be performed in clinics, at the patient bedside, or in a dedicated hospital room.

2. Experimental

2.1. Chemicals, solutions and sample preparation

A 2 mM MTX (≥98%) stock solution was prepared by dissolving the powder in 10 μL NaOH 1 M and then diluting this solution with phosphate buffered saline (PBS) pH 7.4. This solution was aliquoted and stored at −20 °C. PBS pH 7.4 was prepared by mixing 0.01 M disodium phosphate (Na_2HPO_4), 0.002 M monopotassium phosphate (KH_2PO_4), 0.0027 M potassium chloride (KCl), and 0.137 M sodium chloride (NaCl). Human serum (from male AB plasma) was spiked with MTX stock solution and was used to build calibration curves.

All chemicals were purchased from Sigma-Aldrich (Merck, Darmstadt, Germany) and were of analytical grade. Unless otherwise stated, all solutions were prepared with ultra-pure water (18.2 MΩcm, Milli-Q purification device, Millipore Corporation, Billerica, MA, USA).

Patient serum samples from children undergoing HD-MTX therapy were provided by Rigshospitalet, Copenhagen, Denmark ($n = 9$). Two samples were provided for each patient: a sample drawn just before starting MTX infusion (T0) and samples collected 23 h after the start of MTX infusion (T23) as part of the standard protocol used at the hospital (ethical committee approval number: Capital Region Ethics Committee no H-13005724).

2.2. Fabrication of Ag-coated nanopillar SERS substrates

Silver-coated silicon nanopillars (AgNPs) were fabricated using a 2-step process, as previously described in Göksel et al. [30] In short, single-side polished 4silicon wafers (Siegert Wafer GmbH, Aachen, Germany) were etched using a reactive ion etching (RIE) process, leading to the formation of silica NPs of approximately 400 nm in height, 50 nm in width and with a density of approximately 20 NPs/μm^2. A 1 min oxygen plasma cleaning step was performed, before deposition of a 225 nm silver layer on the NPs at a rate of 5 Å/s (Temescal FC-2000, Ferrotec, Livermore, CA, USA). The SERS wafers were diced with a laser micromachining tool (D-09126, 3D-Micromac AG, Chemnitz, Germany) into 4 × 4 mm^2 chips and stored under vacuum until further use.

2.3. Sample preparation

As reported earlier [12], an SPE method was used in a syringe filter, briefly 65 mg of Oasis HLB 30 μm sorbent (Waters, Milford, MA, USA) were left overnight in 1 mL of a 50/50 (*v*/v) mixture of water/methanol. This suspension was then vortexed and quickly inserted in a syringe filter with a cellulose acetate membrane (0.22 μm pore size, Q-Max 25 mm diameter, Frisenette). Then, 0.1 mL of patient sample was previously diluted with 0.9 mL of commercial serum and 4 mL of water (for 23 h patient samples) and loaded onto the filter at a 1 mL/min speed. For the calibration curve, 1 mL commercial serum spiked with MTX was diluted with 4 mL of water and loaded onto the filter (1 mL/min). The sorbent was then quickly washed with 1 mL of 5% methanol in water. Finally, MTX was desorbed with 500 μL methanol (1 mL/min, 4 desorption cycles).

2.4. SERS measurements

SERS measurements were conducted on an in-house built tabletop spectrophotometer (25 × 30 × 30 cm^3, 7 kg), equipped with a 785 nm laser (450 mW, ~120 μm spot size on the sample) and a 25 μm slit [31]. The laser power and exposure time were set to 75 mW and 100 ms, respectively. The entire SERS chip was mapped, with a 100 μm step size.

55 μL of sample collected after SPE were pipetted in the cap of a 200 μL microcentrifuge tube (Saratedt AG & Co. KG, Germany). The 5% extremity of the SERS chip was dipped into the sample for 1 min and left to dry before analysis.

2.5. Chromatographic method

A reverse-phase HPLC method was developed as a reference method on a Shimadzu Prominence HPLC system (Shimadzu, Kyoto, Japan) equipped with an auto-sampler (SIL-20 A, Shimadzu, Kyoto, Japan) and a photo-diode array (PDA) detector (SPD-M20A, Shimadzu, Kyoto, Japan). The stationary phase consisted of a C_{18} column (2.1 × 250 mm, 5 μm) with a guard column (C_{18}, 4.6 × 12.5 mm, 5 μm, 95 Å, 400 bar pressure limit), both from Agilent Technologies (Santa Clara, CA, USA). The column was heated at 40 °C. The mobile phase was a mixture of PBS pH 2 and acetonitrile (83:17 *v*/v) in isocratic mode, at a 0.5 mL/min

flow rate. The pH of the buffer was adjusted to pH 2 with hydrochloric acid (37%). The sample injection volume was 30 µL and MTX peak was observed at 303 nm at a retention time of approximately 11.2 min.

Serum sample clean-up was performed by protein precipitation. 200 µL of methanol were added to 100 µL of sample, and the resulting mixture was vortexed for 1 min before being centrifuged for 5 min at 5000 rpm. The supernatant was analyzed by HPLC.

2.6. Data analysis

SERS data were analyzed with an in-house developed analysis software combining Delphi RAD Studio (Embarcadero Technologies, Austin, TX, USA) and Python (Python Software Foundation, Wilmington, DE, USA) [31]. The spectra were cropped between 600 and 1500 cm^{-1}, and the baseline was corrected using a rolling-circle filter (radius of 100, ellipticity of 6). The average spectrum was extracted from the 20% pixels showing the highest intensity at 680 or 1366 cm^{-1} in each map. The peak height at 680 or 1366 cm^{-1} was used for univariate analysis, while PLSR (2 latent variables, cross-validation with Venetian blinds) was applied for multivariate data analysis.

The limit of detection (LoD) was calculated by 3σ/s (with σ the standard deviation of blank samples and s the slope of the calibration curve), and the limit of quantification (LoQ) was obtained by multiplying the LoD by 3.3. For HPLC calibration data, the LoD was instead calculated using the standard deviation of the intercept as σ. Origin 2021 (OriginLab Corporation, Northampton, MA, USA) was used to plot all data. Matlab (2021b, MathWorks, Natick, MA, USA) and the PLS Toolbox (Eigenvector research, Manson, WA, USA) were used for multivariate data analysis. All the figures of merit of the PLSR, including LoD and LoQ, were obtained from the MVC toolbox in Matlab. A statistical analysis (*t*-test, correlation analysis) was conducted using Microsoft Excel 2016 (Microsoft Corporation, Redmond, WA, USA). If not otherwise specified, all data was analyzed at least in triplicates.

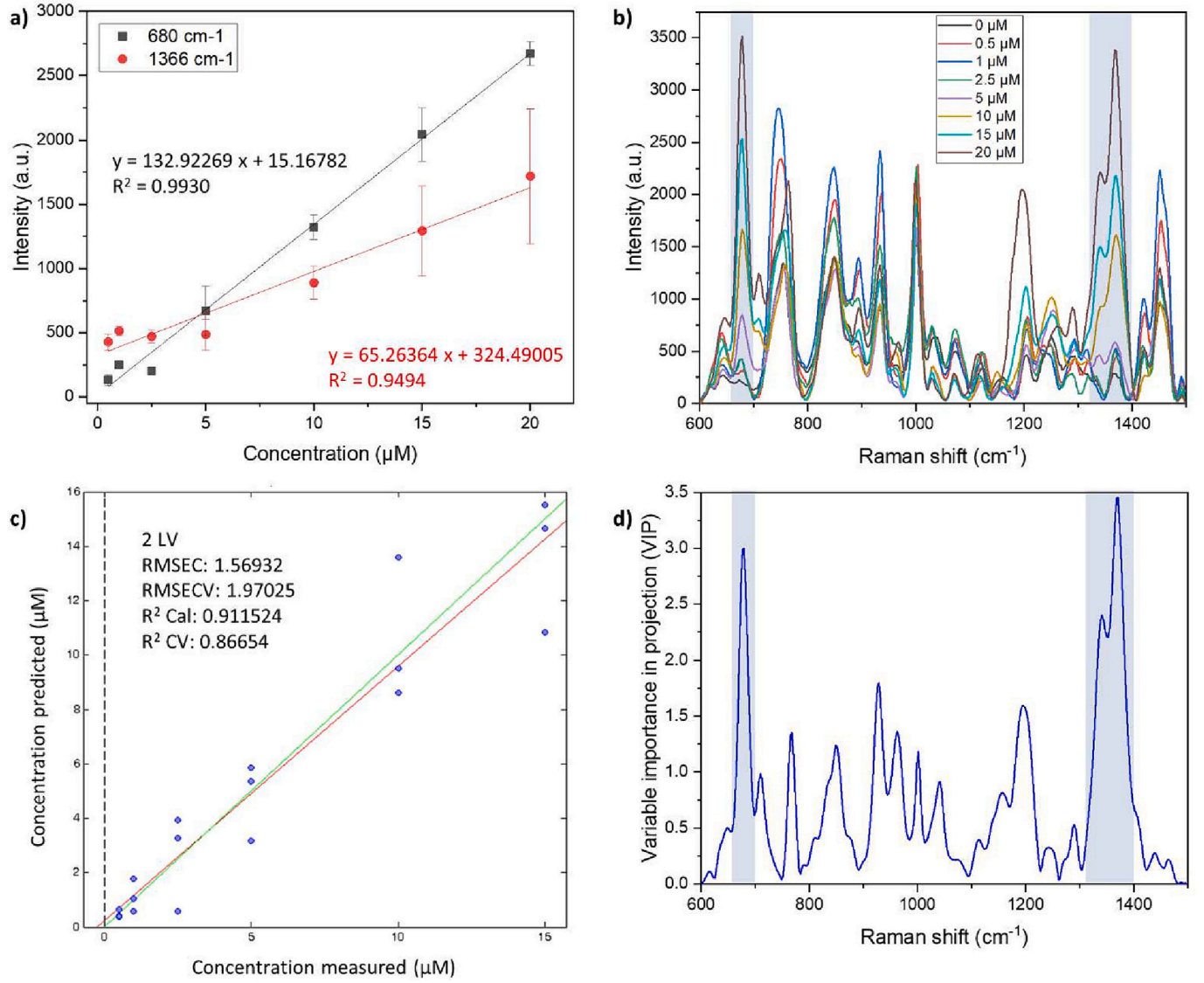

Fig. 1. Univariate calibration curves built using MTX characteristic peak height at 680 cm^{-1} (black squares) or at 1366 cm^{-1} (red dots) (a) and the corresponding SERS spectra (b). PLSR model constructed with 2 latent variables on SERS data of serum samples after SPE (c), and plot of the variable importance in projection (VIP) of the PLSR model (d). The light blue rectangles in b) and d) highlight the main characteristic MTX peaks, located at 680 and 1366 cm^{-1}. (For interpretation of the references to colour in this figure legend, the reader is referred to the web version of this article.)

3. Results and discussion

3.1. SERS-based MTX quantification

Serum matrices are complex and require a certain amount of sample clean-up to be compatible with SERS analysis [12,30,31]. Previously, we have demonstrated that SPE is well-suited to this purpose, combining efficient sample clean-up and up-concentration [12]. Moreover, we have previously developed a NPAS sampling method that enables further sample cleaning by allowing sample migration and separation on the SERS substrate [12,30].

A similar sample pre-treatment approach reported earlier [12] was used to build an MTX quantification model, using commercial serum samples spiked with MTX, to be used as the calibration curve for quantifying the patient samples. Previously, we also demonstrated that the use of chemometrics enabled quantification of patient samples from a calibration curve built using commercial serum samples [32].

The performance of univariate quantification models (Fig. 1a) built using the most prominent characteristic peaks of MTX, namely 680 or 1366 cm^{-1} (Fig. 1b), were compared to a multivariate data analysis model based on PLSR (Fig. 1c).

In both cases of univariate calibration, good linearity was obtained between the peak height and MTX concentration in the 0.5–20 μM range (R^2 of 0.9930 and 0.9494, for calibration curves built using 680 and 1366 cm^{-1} peak height, respectively, $p < 0.001$ in both cases). The LoD and LoQ were calculated as 0.35 μM and 1.16 μM (680 cm^{-1} calibration) and 0.36 μM and 1.18 μM (1366 cm^{-1} calibration), respectively. However, it can be observed in Fig. 1a and b that the slopes of those two calibration curves were very different and that a matrix effect was observed for the 1366 cm^{-1} univariate calibration.

In comparison, the multivariate PLSR model showed good linearity over the 0.5–20 μM range (R^2 of 0.9115), which would be suitable for the quantification of the expected concentration in the serum sample, with calculated LoD and LoQ of 2.87 and 8.62 μM, respectively. Even though those values are higher, multivariate data analysis is nonetheless more robust to sample variability than univariate analysis [12,32]. Furthermore, the analytical sensitivity was calculated for the 2 univariate models and for the multivariate one. The analytical sensitivity was much higher in the case of PLSR (5.59 μM^{-1}) than for the univariate models, with the univariate model built using 680 cm^{-1} displaying a higher analytical sensitivity than for the model built with 1366 cm^{-1} (1.38 vs. 0.36 μM^{-1}, respectively). This suggests that the PLSR model is more sensitive than the univariate ones.

The variable importance in projection (VIP) of the PLSR is displayed in Fig. 1d. As it can be observed, the main bands contributing to the PLSR model, i.e., having the highest VIP values, are the characteristic MTX bands located at 680 and 1366 cm^{-1} (highlighted by light blue rectangles in Fig. 1d). However, there are additional variables whose VIP score is superior to 1, and that, therefore, contribute to the PLSR model. Those are located at 767, 849, 929, 962, 1001 and 1195 cm^{-1}. The latent variables of the PLSR model are displayed in Fig. S1.

The spatial distribution of the 680 cm^{-1} MTX peak on the SERS substrate, depending on MTX concentration, is illustrated in Fig. S2. It was observed that MTX migrated preferentially to the top part of the SERS chip. When increasing the concentration, the distribution of MTX was more spread over the SERS chip surface.

3.2. HPLC reference method

To evaluate the analytical performance of the SERS-based MTX quantification from patient samples, a reverse-phase isocratic HPLC-PDA method was developed, based on and adapted from [33,34]. Chromatography is the reference method for MTX detection from patient samples, as, due to its high selectivity, it can separate MTX from other structurally related metabolites, such as 2,4-diamino-N10-methylpteroic acid (DAMPA) or 7-hydroxymethotrexate (7-OH MTX), that can interfere with immunoassays through cross-reactivity with the antibodies used [4].

Commercial serum was spiked with a reference stock MTX solution, leading to final solutions containing between 0.2 and 150 μM MTX. Those samples were cleaned with a simple protein precipitation step and then analyzed with the developed HPLC method. Protein precipitation was selected as a fast and easy pre-treatment method. A linear relationship was observed (R^2 of 0.9867) between the spiked MTX concentration and the area under MTX peak, at the retention time of 11.2 min (Fig. 2, black curve). The calculated LoD and LoQ were 7.92 and 26.15 μM, respectively. In addition, the intra-day RSD was 7.02% (calculated on the whole concentration range) and the inter-day RSD was 8.62% (calculated on the 25 μM concentration point). A patient sample free of MTX was also spiked with 25 μM and analyzed, and the obtained recovery was 121.21%.

The influence of the SPE procedure was investigated by analyzing commercial serum samples spiked with a known amount of MTX, ranging from 0.5 μM to 20 μM, and cleaned up by SPE, with the developed HPLC method (Fig. 2, red curve). Linearity was observed between MTX peak area and concentrations (R^2 of 0.9982) and the LoD and LoQ were calculated to be 1.07 and 3.54 μM, respectively. Considering the 2× up-concentration introduced during the SPE procedure (loading of 1 mL sample vs. desorption with 500 μL methanol), a higher sensitivity was observed for serum samples pre-treated by SPE than with protein precipitation. This could be due to the fact that MTX is highly bound to proteins (around 95%) [35], and that SPE could be more efficient freeing MTX from proteins.

The analytical sensitivity was calculated for those two approaches using the developed chromatographic method. The calibration curve built with samples prepared by SPE had a higher analytical sensitivity than the one constructed with protein-precipitated samples (1.91 vs. 0.37 μM^{-1}, respectively), highlighting a better sensitivity of the calibration curve based on SPE-processed samples.

A chromatogram from a patient sample (containing around 80 μm MTX) after protein precipitation and after SPE is displayed in Fig. S3. It can be observed that the chromatogram of the protein precipitated sample contains more peaks than the one from SPE, suggesting the presence of more matrix components in the protein precipitated samples and a better sample clean-up by SPE [36]. This is also in accordance with

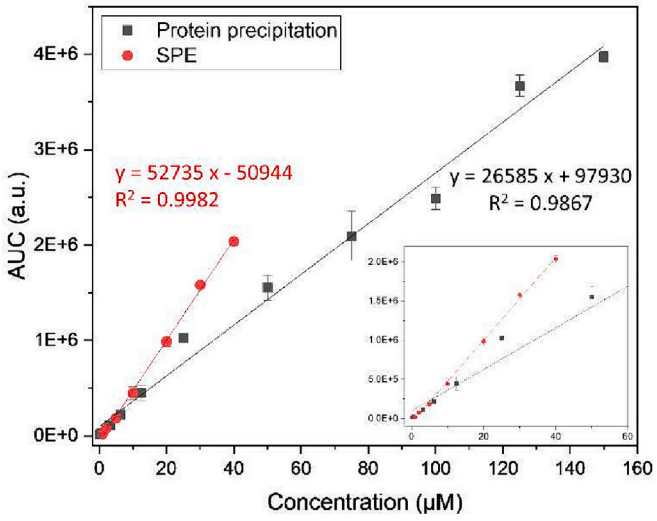

Fig. 2. Comparison of the calibration curves obtained by HPLC after protein precipitation (black squares and black curve) and after SPE (red dots and red curve), indicating a higher extraction efficiency for SPE. The lower concentration region is enlarged in the inset. (For interpretation of the references to colour in this figure legend, the reader is referred to the web version of this article.)

the fact that a lower slope was obtained in the calibration curve built with protein-precipitated samples, implying more matrix effect for protein precipitation than for SPE. While this is not an issue for HPLC analysis, it can explain why the sensitivity of samples pre-treated with SPE and analyzed with SERS is higher than the one treated with protein precipitation [30,32]. SERS is indeed very susceptible to surface fouling by matrix components present in the sample, which can reduce the method sensitivity [24,25].

3.3. Method comparison

Patient serum samples, collected 23 h after the start of MTX infusion during HD-MTX therapy, were then analyzed, and their concentration was estimated using the calibration curves previously built. Since the MTX concentrations in those samples were above the highest limit of the linear range of the developed SERS method, they were diluted 10× with commercial serum, which further benefited the SERS detection by decreasing the complexity of the matrix. The diluted samples were closer to the commercial serum composition, reducing the biological variability between patient serum samples.

Comparison between the developed SERS method and the reference HPLC was done using a scatter plot and a difference (Bland-Altman) plot [18,37,38]. Results from both HPLC using protein precipitation and SPE as sample pre-treatment were used, while the test method was limited to SERS combined with PLSR, since multivariate data analysis is more robust to the variability that can arise from biological samples [12].

As it can be observed in Fig. 3, a good correlation was observed between the SERS-based (test method) and the reference methods, with 'Pearson's correlation coefficients of 0.8228 ($p < 0.05$) and 0.8888 ($p < 0.005$) for the protein precipitation-HPLC and SPE-HPLC, respectively. In addition, *t*-tests conducted on each sample, comparing the chromatographic methods with SERS, resulted in *p*-values higher than 0.05, implying insufficient evidence to claim a significant difference between the results obtained with SERS and with HPLC (Fig. S4). Only one sample in the protein precipitation-HPLC vs. SERS comparison showed a p-value below 0.05 (Fig. S4, sample 1). A better correlation was observed between the SPE-HPLC and the SERS methods, which is not surprising since the extraction efficiency of the protein precipitation method was lower than the SPE one (Fig. 2), and SPE was the sample preparation method used both for SERS and HPLC.

The SERS-based method underestimated MTX concentration compared to the HPLC ones, and a 10% bias was calculated (Fig. 4, solid black line). All the samples analyzed were located within the 95% limits of agreement (Fig. 3). Moreover, the variability of the SERS and HPLC measurements with SPE sample pre-treatment was similar, around 10% (RSD of 8.4% for HPLC and 11.6% for SERS, Fig. S5) while the variability of the PP-HPLC method was lower (RSD of 5.1%, Fig. S5), probably due to the fact that this sample pre-treatment method is simpler and comprises less steps.

Overall, comparison with a reference chromatographic method shows a robust correlation between the SERS assay and the established technique. Despite a 10% bias in the SERS-based approach, both methods demonstrated similar variability. These findings highlight the potential accuracy and precision of the SERS assay in TDM of MTX, laying the groundwork for its clinical implementation.

4. Conclusions

In this paper, a label-free SERS-based assay was used on a benchtop device, to quantify MTX from samples originating from patients undergoing HD-MTX therapy. The assay combined SPE sample pre-treatment with PLSR multivariate data analysis to overcome sample matrix complexity and variability. Statistical analysis of the data demonstrated a good correlation between the gold standard HPLC method and the developed label-free SERS approach. The results provided in this paper represent the first step towards a full clinical validation of a quantitative SERS-based assay for TDM that could be performed in a point-of-need setting. We believe that the developed SERS-based assay could be ground-breaking for TDM of HD-MTX in low- and middle-income countries, where access to reference methods is restricted. To extend the applicability of the assay to lower MTX concentration measurements (< 0.5 μM), improvement of the sample pre-treatment will further be investigated.

CRediT authorship contribution statement

Elodie Dumont: Writing – review & editing, Writing – original draft, Methodology, Formal analysis, Data curation, Conceptualization. **Gohar Soufi:** Writing – review & editing, Writing – original draft, Methodology, Investigation, Formal analysis, Data curation, Conceptualization.

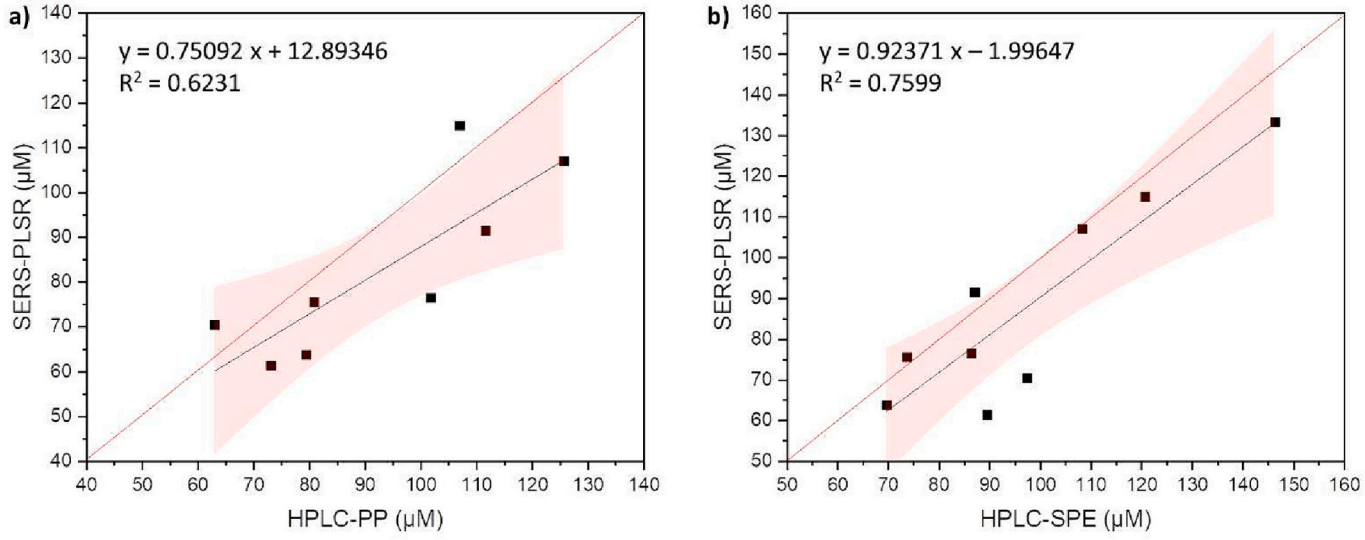

Fig. 3. Scatter plot built using HPLC with protein precipitation (PP) (a) or with SPE (b) as reference method, and the developed SERS method combined with PLSR multivariate data analysis as test method. The black and red lines represent the regression line and the line of identity, respectively, while the 95% confidence band is depicted as red area. The Pearson correlation coefficient (r) is 0.8228 ($p < 0.05$) in a) and 0.8888 ($p < 0.005$) in b). (For interpretation of the references to colour in this figure legend, the reader is referred to the web version of this article.)

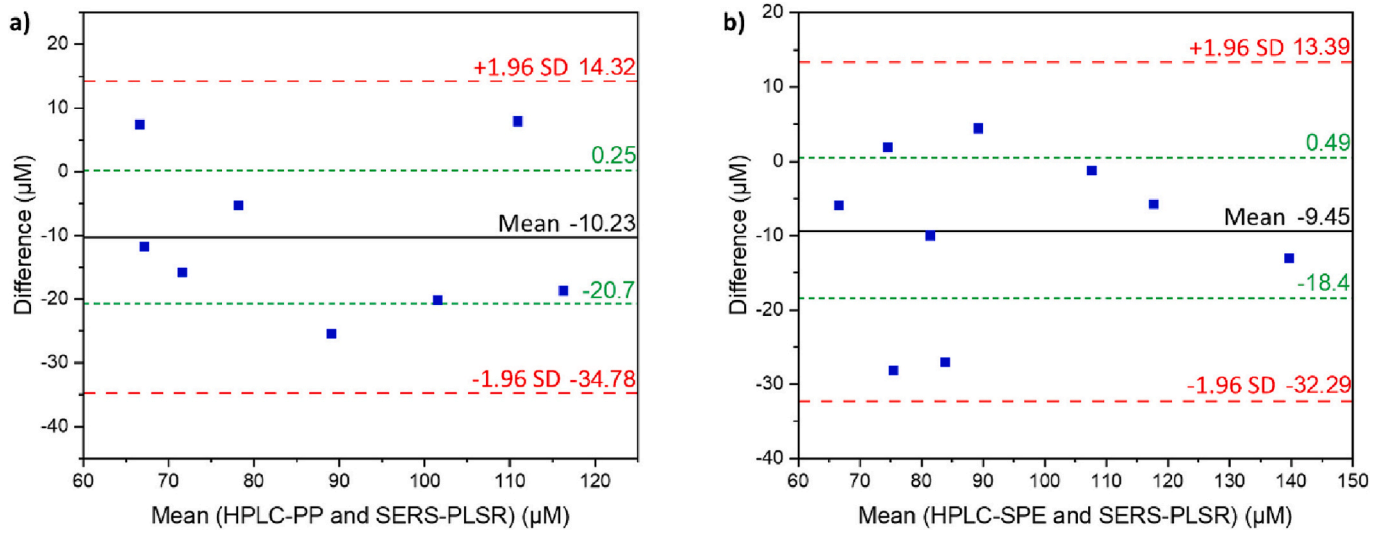

Fig. 4. Bland-Altman plot built using HPLC with protein precipitation (a) or with SPE (b) as reference method, and the developed SERS method combined with PLSR multivariate data analysis as test method. The solid black and short-dashed green and dashed red lines represent the mean (bias), 95% confidence interval on the mean, and 95% limits of agreement, respectively. (For interpretation of the references to colour in this figure legend, the reader is referred to the web version of this article.)

Yaman Göksel: Visualization, Formal analysis, Data curation. **Roman Slipets:** Software. **Raheel Altaf Raja:** Writing – review & editing, Validation. **Kjeld Schmiegelow:** Writing – review & editing, Validation, Funding acquisition. **Kinga Zor:** Writing – original draft, Supervision, Conceptualization. **Anja Boisen:** Writing – review & editing, Supervision, Project administration, Funding acquisition.

Declaration of competing interest

There are no conflicts to declare.

Data availability

Data will be made available on request.

Acknowledgements

ED acknowledges Lasse H. E. Thamdrup for SERS substrate fabrication and characterization. ED, GS, YG, RS, KZ and AB acknowledge financial support from the Danish National Research Foundation (DNRF122), Villum Fonden (Grant no. 9301) for Intelligent Drug delivery and sensing Using microcontainers and Nanomechanics (IDUN) and BioInnovation Institute Foundation for Therapeutic drug monitoring (Grant no. NNF20SA0063552). AB acknowledges financial support from Danish Childhood Cancer Foundation (Grant no 2023-001089). KS acknowledges financial support from Danish Cancer Society (grant no R257-A14720) and Danish Childhood Cancer Foundation (Grants no 2019-5934 and 2020-6759).

Appendix A. Supplementary data

Supplementary data to this article can be found online at https://doi.org/10.1016/j.sbsr.2024.100649.

References

[1] K. Vaishnavi, D. Bansal, A. Trehan, R. Jain, S.V. Attri, Pediatr. Blood Cancer 65 (2018) e27241.
[2] L.B. Ramsey, F.M. Balis, M.M. O'Brien, K. Schmiegelow, J.L. Pauley, A. Bleyer, B. C. Widemann, D. Askenazi, S. Bergeron, A. Shirali, S. Schwartz, A.A. Vinks, J. Heldrup, Oncologist 23 (2018) 52–61.
[3] T.V.Ch. Skärby, H. Anderson, J. Heldrup, J.A. Kanerva, K. Schmiegelow, Leukemia 20 (2006), 1995–1962.
[4] J. Descoeur, A.M. Dupuy, A.S. Bargnoux, J.P. Cristol, O. Mathieu, J. Oncol. Pharm. Pract. 28 (2022) 55–63.
[5] Cobas® 8000 modular analyzer series. https://diagnostics.roche.com/global/en/products/systems/cobas-8000-analyzer-series-sys-128.html accessed 28 November 2023.
[6] ARK™ Methotrexate Assay (Trexall®). https://ark-tdm.com/products/cancer/methotrexate/index.html.
[7] P.S. Agogo-Mawuli, D. P., Siderovski, in: S.K. Amponsah, Y.V. Pathak (Eds.), Recent Advances in Therapeutic Drug Monitoring and Clinical Toxicology, Springer, Cham, 2022, pp. 233–253.
[8] S.K. Amponsah, Y.V. Pathak, in: S.K. Amponsah, Y.V. Pathak (Eds.), Recent Advances in Therapeutic Drug Monitoring and Clinical Toxicology, Springer, Cham, 2022, pp. 369–377.
[9] B. Basu, B.G. Prajapati, S. Mukherjee, T.K. Roy, A. Roy, C.M. Hossain, J. B. Prajapati, J. Patel, in: S.K. Amponsah, Y.V. Pathak (Eds.), Recent Advances in Therapeutic Drug Monitoring and Clinical Toxicology, Springer, Cham, 2022, pp. 95–116.
[10] M. Parrilla, U. Detamornrat, J. Domínguez-Robles, S. Tunca, R.F. Donnelly, K. De Wael, ACS Sens. 8 (2023) 4161–4170.
[11] C. Liu, S. Weber, R. Peng, L. Wu, W. Shu Zhang, P.B. Luppa, J. Popp, D. Cialla-May, TrAC - Trends Anal. Chem. 164 (2023) 117094.
[12] G. Soufi, E. Dumont, Y. Göksel, R. Slipets, R.A. Raja, K. Schmiegelow, H. Bagheri, A. Boisen, K. Zor, Biosens. Bioelectron. X 14 (2023) 1–10.
[13] H. Chon, R. Wang, S. Lee, S.Y. Bang, H.S. Lee, S.C. Bae, S.H. Hong, Y.H. Yoon, D. W. Lim, A.J. DeMello, J. Choo, Anal. Bioanal. Chem. 407 (2015) 8353–8362.
[14] M. Feizpour, Q. Liu, T. Van der Donck, H. Thienpont, W. Meulebroeck, H. Ottevaere, J. Phys. Photonics. 6 (2024) 025002.
[15] N.E. Markina, I.Y. Goryacheva, A.V. Markin, Colloids Interf. 7 (2023) 42.
[16] N.E. Markina, A.M. Zakharevich, A.V. Markin, Anal. Bioanal. Chem. 412 (2020) 7757–7766.
[17] C. Muehlethaler, M. Leona, J.R. Lombardi, Forensic Sci. Int. 268 (2016) 1–13.
[18] J. Pum, A Practical Guide to Validation and Verification of Analytical Methods in the Clinical Laboratory 1st edn, vol. 90, Elsevier Inc., 2019.
[19] S. Chandran, R.S.P. Singh, Pharmazie 62 (2007) 4–14.
[20] B.P. Booth, W.C. Simon, In New Drug Development: Regulatory Paradigms for Clinical Pharmacology and Biopharmaceutics, CRC Press, Boca Raton, FL, USA, 2016, pp. 138–159.
[21] K.M. Koo, J. Wang, R.S. Richards, A. Farrell, J.W. Yaxley, H. Samaratunga, P. E. Teloken, M.J. Roberts, G.D. Coughlin, M.F. Lavin, P.N. Mainwaring, Y. Wang, R. A. Gardiner, M. Trau, ACS Nano 12 (2018) 8362–8371.
[22] B. Bilgin, H. Torun, M. Ilgü, C. Yanik, S.N. Batur, S. Çelik, M. Öztürk, Ö. Dogan, Ö. Ergönül, I. Solaroglu, F. Can, M.C. Onbasli, Proceed. SPIE 11957 (2022) 1195708.
[23] L. Wu, A. Teixeira, A. Garrido-Maestu, L. Muinelo-Romay, L. Lima, L.L. Santos, M. Prado, L. Diéguez, Biosens. Bioelectron. 165 (2020) 112392.
[24] R. Haldavnekar, S. Ganesh, K. Venkatakrishnan, B. Tan, Small Methods 6 (2022) 1–21.
[25] W.H. Kim, J.U. Lee, M.J. Jeon, K.H. Park, S.J. Sim, Biosens. Bioelectron. 205 (2022) 114116.
[26] C. Zong, M. Xu, L.J. Xu, T. Wei, X. Ma, X.S. Zheng, R. Hu, B. Ren, Chem. Rev. 118 (2018) 4946–4980.

[27] A., in: Y. Wang (Ed.), Bonifacio, in Principles and Clinical Diagnostic Applications of Surface-Enhanced Raman Spectroscopy, Elsevier Inc., 2022, pp. 125–170.
[28] E. Dumont, C. De Bleye, G. Rademaker, L. Coïc, J. Horne, P.Y. Sacré, O. Peulen, P. Hubert, E. Ziemons, Talanta 224 (2021) 121866.
[29] S.S. Panikar, D. Cialla-May, E. De la Rosa, P. Salas, J. Popp, TrAC - Trends Anal. Chem. 134 (2021) 116122.
[30] Y. Göksel, K. Zor, T. Rindzevicius, B.E. Thorhauge Als-Nielsen, K. Schmiegelow, A. Boisen, ACS Sens. 6 (2021) 2664–2673.
[31] Y. Göksel, E. Dumont, R. Slipets, S.T. Rajendran, S. Sarikaya, L.H.E. Thamdrup, K. Schmiegelow, T. Rindzevicius, K. Zor, A. Boisen, ACS Sens. 7 (2022) 2358–2369.
[32] P. He, E. Dumont, Y. Göksel, R. Slipets, K. Schmiegelow, Q. Chen, K. Zor, A. Boisen, Spectrochim., Acta - Part A Mol. Biomol. Spectrosc. 305 (2024) 123536.
[33] P. Koufopantelis, S. Georgakakou, M. Kazanis, C. Giaginis, A. Margeli, S. Papargiri, I. Panderi, J. Chromatogr. B Anal. Technol. Biomed. Life Sci. 877 (2009) 3850–3856.
[34] Y.D. Li, Y. Li, N.S. Liang, F. Yang, Z.P. Kuang, J. Chromatogr. B Anal. Technol. Biomed. Life Sci. 1002 (2015) 107–112.
[35] W.H. Steele, J.R. Lawrence, J.F.B. Stuart, C.A. McNeill, Eur. J. Clin. Pharmacol. 15 (1979) 363–366.
[36] J.J. Zheng, E.D. Lynch, S.E. Unger, J. Pharm. Biomed. Anal. 28 (2002) 279–285.
[37] J.P.J. Ungerer, C.J. Pretorius, Clin. Chem. Lab. Med. 56 (2017) 1–4.
[38] D. Giavarina, Biochem. Med. 25 (2015) 141–151.